Publication Year	2016
Acceptance in OA	2020-05-14T14:28:53Z
Title	The accretion regimes of a highly magnetized NS: the unique case of NuSTAR J095551+6940.8
Authors	DALL'OSSO, Simone, Perna, Rosalba, PAPITTO, ALESSANDRO, Bozzo, Enrico, STELLA, Luigi
Publisher's version (DOI)	10.1093/mnras/stw110
Handle	http://hdl.handle.net/20.500.12386/24823
Journal	MONTHLY NOTICES OF THE ROYAL ASTRONOMICAL SOCIETY
Volume	457

Monthly Notices of the ROYAL ASTRONOMICAL SOCIETY
MNRAS **457,** 3076–3083 (2016) doi:10.1093/mnras/stw110

The accretion regimes of a highly magnetized NS: the unique case of NuSTAR J095551+6940.8

Simone Dall'Osso,[1]★ Rosalba Perna,[1] Alessandro Papitto,[2] Enrico Bozzo[3] and Luigi Stella[4]

[1]*Department of Physics and Astronomy, Stony Brook University, Stony Brook, NY 11794-3391, USA*
[2]*Institute of Space Sciences (ICE, CSICIEEC), Carrer de Can Magrans, S/N, E-08193 Barcelona, Spain*
[3]*ISDC, University of Geneva, Chemin d'Ecogia 16, CH-1290 Versoix, Switzerland*
[4]*INAF – Osservatorio Astronomico di Roma, via di Frascati 33, I-00044 Monteporzio Catone, Roma, Italy*

Accepted 2016 January 8. Received 2016 January 6; in original form 2015 November 30

ABSTRACT

The ultraluminous accreting pulsar M82-X2 (NuSTAR J095551+6940.8) offers an unprecedented opportunity to study the disc-magnetosphere interaction in a new regime of supercritical accretion. The source X-ray emission has been highly variable during the last 15 yrs. It ranged from a maximum of $\sim 2 \times 10^{40}$ erg s^{-1} through intermediate values $\sim$ a few $\times 10^{39}$ erg s^{-1}, and down to a minimum below 2×10^{38} erg s^{-1} that we have determined here, by analysing archival Chandra HRC observations of the source at an epoch at which it was undetected. We interpret the source variability via a magnetically threaded disc model: when at peak luminosity, the neutron star (NS) is close to spin equilibrium, its inner disc edge $r_m \sim 10^8$ cm is approximately half the corotation radius $r_{\rm co}$, and radiation pressure dominates the disc out to $r_{\rm tr} \lesssim 10^9$ cm. In the radiation-pressure-dominated regime, r_m grows very slowly as the mass inflow rate drops: as a result, $r_m < r_{\rm co}$ remains valid until $\dot{M} \gtrsim \dot{M}_E$, the Eddington accretion rate, allowing a wide range of accretion luminosities to the NS. Once $\dot{M} < \dot{M}_E$ accretion on to the NS is inhibited because $r_m > r_{\rm co}$, and the source luminosity is expected to drop by a large factor. We conclude that a magnetically threaded accretion disc surrounding a highly magnetized NS ($B \lesssim 10^{13}$ G), and transitioning between the radiation-pressure and gas-pressure dominated regimes, offers the best interpretation for all the currently observed properties of NuSTAR J095551+6940.8.

Key words: accretion, accretion discs – stars: magnetic field – stars: neutron – pulsars: general.

1 INTRODUCTION

The discovery by *NuSTAR* (Bachetti et al. 2014) of coherent pulsations in the X-ray emission of an Ultra-Luminous X-ray source (ULX) has challenged our understanding of both ULXs as well as of accretion on to magnetized neutron stars (NSs). The source, observed at a peak X-ray luminosity $L_{\rm X}$ of $\sim 10^{40}$ erg s^{-1} (assuming isotropic emission) has triggered numerous studies aimed at discerning its nature and properties, and in particular the magnetic field strength of the accreting NS in it.

The early works, based on the value of the luminosity in this 'high state', reached however conclusions which were not univocal. In particular, a magnetar-like magnetic field of $\sim 10^{14}$ G was derived by Eksi et al. (2015), while Lyutikov (2014) favoured a B-field $\sim 10^{13}$ G. A more 'typical' NS field of 10^{12} G was suggested by the analysis of Christodoulou, Laycock & Kazanas (2014; see also Bachetti et al. 2014), while Kluzniak & Lasota (2015) argued in favour of a very low field, $< 10^9$ G. A mixed magnetic field topology, with a low dipolar field and magnetar-strength multipoles was envisaged by Tong (2015). These different conclusions stemmed from the combination of different assumptions: i.e. isotropic emission versus beamed, spin equilibrium or else purely material accretion torques versus magnetically threaded discs.

In Dall'Osso, Perna & Stella (2015, paper I from here on), we analysed the source properties by considering a magnetically threaded disc without prior assumptions on how close the NS is to spin equilibrium. First, we used the average value of the period derivative $\dot{P}$ (over four sets of observations) to show that there exists a continuum of solutions in the B versus $\dot{M}$ (or $L_{\rm X}$) plane, and that the solutions found by previous investigators correspond to particular cases of the more general solution. Secondly, we

★ E-mail: sim.dall@gmail.com

© 2016 The Authors
Published by Oxford University Press on behalf of the Royal Astronomical Society

Downloaded from https://academic.oup.com/mnras/article-abstract/457/3/3076/2588907 by guest on 29 April 2020

included in the analysis the observed $\dot{P}$ variations to show that only high-field solutions, corresponding to $B \gtrsim 10^{13}$ G, could account for those fluctuations (over four time intervals) without requiring major changes in $\dot{M}$, which would be at odds with the approximately constant X-ray emission of the source during the same time.

All these works relied on the NuSTAR J095551+6940.8 observations (Bachetti et al. 2014) of the source in its 'high' state, with $L_X \sim 10^{40}$ erg s^{-1}. However, an analysis of archival *Chandra* data over a period of 15 yr by Brightman et al. (2016) revealed that the source can be found in several accretion states, with large luminosity variations, down to $L_X \sim 10^{38}$ erg s^{-1}. In addition, Brightman et al. used *NuSTAR* data to study the spectrum of the pulsed component. They found it broadly consistent with typical spectra of accreting pulsars in High Mass X-ray Binaries. These archival *Chandra* observations were analysed also by Tsygankov et al. (2016), who suggested a possible bimodal distribution of the luminosity, with two well-defined peaks separated by a factor ~ 40. They interpreted this bimodality as due to transitions between the accretion and the propeller phase in a NS with a magnetic field $\sim 10^{14}$ G.

Here, we begin by performing an analysis of two archival *Chandra*/High Resolution Camera (HRC) observations which were not previously published due to lack of spectral information. We show that, in one of those observations, the source was not detected. Hence, over the 15 yr of observations, the source has displayed three states: a high-luminosity one with $L_X \sim 10^{40}$ erg s^{-1}, an intermediate-luminosity one with L_X varying between $\sim$afew $\times 10^{38}$ erg s^{-1} to a few $\times 10^{39}$ erg s^{-1}, and a low-luminosity one with an upper limit of $L_X < 2 \times 10^{38}$ erg s^{-1} (see Section 2). These luminosity variations, which encompass the Eddington limit, also straddle the regime in which the inner disc transitions from being pressure dominated to radiation dominated. As such, the source NuSTAR J095551+6940.8 offers an unprecedented opportunity to study accretion on to a magnetized NS across a wide range of physical conditions. Such a study is the goal of this work.

The paper is organized as follows: Section 2 describes the analysis of the relevant HRC *Chandra* data (where the source is not detected); Section 3 summarizes the basics of the threaded disc model, both in the gas and in the radiation-dominated regimes. The direct application to NuSTAR J095551+6940.8is presented in Section 4 for a wide range of different models. We summarize and conclude in Section 5.

2 *CHANDRA* ARCHIVAL OBSERVATIONS: SETTING A LIMIT ON THE LOWEST LUMINOSITY OF THE SOURCE

Brightman et al. (2016) analysed *Chandra* archival observations covering a 15 yr period. A few of them were discarded either due to excessive contamination from nearby sources, or because no spectral information was available from the two unpublished long observations made with the HRC only. In the majority of the remaining cases, M82-X2 was detected revealing large flux variations, with the corresponding isotropic luminosity ranging from[1] $L_X \lesssim 10^{40}$ erg s^{-1} to $L_X \gtrsim (2\text{–}3) \times 10^{38}$ erg s^{-1}. For a few observations, Brightman et al. (2016) report detections at luminosities $\sim(1\text{–}2) \times 10^{38}$ erg s^{-1}, albeit with rather large relative errors. In addition to using these, here we also analyse the two long observations made with HRC in order to assess whether the source was actually detected and, if not, set an upper limit on its luminosity.

[1] Different spectral models cause slight luminosity differences.

The HRC observations under consideration were performed on 2007 January 9 (Id. 8189 with a 61.3 ks exposure, Obs. 1 hereafter), and January 12 (Id. 8505 with an 83.2 ks exposure, Obs. 2 hereafter). In both cases *Chandra* observed M82 using the HRC optimized for timing (HRC-S Timing). In order to eliminate mismatches in the absolute astrometry between the two observations, we reprojected them using the HRC *Chandra* image of the source region taken on 1999 October 28, (ObsId. 1411), when the pulsar was bright and we could determine its position relative to other nearby sources. We reduced and analysed data with the Chandra Interactive Analysis of Observations (CIAO) version 4.7, and reprocessed event files using the CHANDRA_REPRO script, with the latest calibration files included in the CALDB v. 4.6.8.

We performed source detection by using the CIAO algorithm WAVDETECT (Freeman et al. 2002), which correlates the *Chandra* image with wavelets of different scales and searches for significant correlations. We searched at scales equal to 1.0, $\sqrt{2}$, 2.0, $2\sqrt{2}$, 4.0, $4\sqrt{2}$, 8.0, $8\sqrt{2}$, and 16.0 times the size of the pixel of HRC-S images (0.13 arcsec); some of these oversample the point spread function of an on axis point source (FWHM$\sim$0.4 arcsec). We chose the sensitivity of the detection algorithm to identify no more than one spurious source within a rectangular field that includes the brightest X-ray sources of the galaxy (see the green dashed box in Fig. 1). That field is $N_{\rm pix} = 100 \times 100$ pixel^2 wide and so the detection threshold was set to a probability $1/N_{\rm pix} = 10^{-4}$ of a spurious detection at the position of M82-X2 (corresponding to a level of $\sim 3.5\sigma$). Fig. 1 shows the image obtained during Obs. 1 (left-hand panel) and Obs. 2 (right-hand panel), respectively. NuSTAR J095551+6940.8 is barely detected, at a significance of 3.9σ, only during Obs. 2 (see the red circle in the right-hand panel of Fig. 1, where the source is dubbed J095551.0, as in table 2 of Chiang & Kong 2011). On the other hand, the source was undetected by WAVDETECT during Obs. 1 (at the 3.5σ confidence level specified above). To estimate the photon counts in the two observations we used the CIAO routine SRCFLUX, extracting photons from a circle with a 0.9 arcsec radius (containing 90 per cent of the counts expected from a point source) centred at the source position. The background was extracted from a larger region far from the centre of the host galaxy. We obtain 0.1–10 keV count rates of $r_1 = (0.92 \pm 0.14) \times 10^{-3}$ and $r_2 = (1.55 \pm 0.15) \times 10^{-3}$ cts s^{-1} in Obs. 1 and 2, respectively.

Although the photon count (63) in Obs. 1 would lead to a detection in the absence of background diffuse emission close to the source position, wavelets at the considered scales did not show a significant correlation with the spatial count distribution. Hence we ascribe most of those counts to the diffuse emission of the galaxy. Indeed, extracting the flux from a circular region located just north-east of the source location yields a count rate of $b_1 = (0.99 \pm 0.13) \times 10^{-3}$ cts s^{-1}, compatible with the flux observed from the position of M82-X2. To study the diffuse emission in the core of M82, we compared the observed flux in a number of different regions (0.75 arcsec radius), centred at positions close to (but not overlapping with) the sources in the core of the galaxy. We found that this diffuse emission varies by up to 70 per cent in magnitude over spatial scales of $\approx$1.5 arcsec, and has an extremely patchy distribution: hence a reliable modelling appears prohibitive with present instrumentation. Therefore, since the relative contribution of the source and the diffuse emission to the observed flux is highly uncertain, we consider the observed values as the most conservative upper limit on the source flux. Adopting the spectral parameters of the high-luminosity state of M82 X-2 (a power law with index $\Gamma = 1.33$ and absorption column of $N_{\rm H} = 3.4 \times 10^{22}$ cm^{-2}; Brightman

Downloaded from https://academic.oup.com/mnras/article-abstract/457/3/3076/2588907 by guest on 29 April 2020

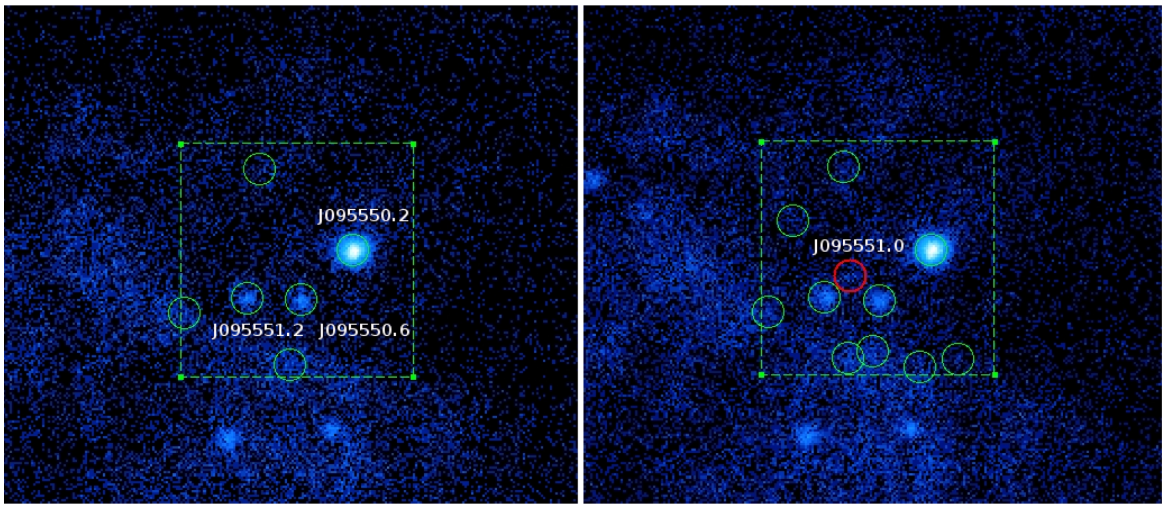

Figure 1. HRC-S image of the core of M82 obtained during Obs. 1 (left-hand panel) and 2 (right-hand panel), respectively. North is to the top of the image and east to the left. Green circles plotted with a radius of 0.9 arcsec indicate sources that were significantly detected by the WAVDETECT algorithm used over the green dashed box. A red circle in the right-hand panel indicates the significant detection of NuSTAR J095551+6940.8.

et al. 2016), the lowest observed count rate, r_1, translates into an unabsorbed (0.1–10) keV flux of 3.4×10^{-13} erg cm^{-2} s^{-1} and a luminosity of 4.4×10^{38} erg s^{-1} (at a distance of 3.3 Mpc; Foley et al. 2014). Alternatively, given that the count rate from the M82-X2 region in Obs. 1 was very close to that in neighbouring source-free regions, we also consider the possibility that r_1 is due to pure background emission. In this case, with a total background of 63 photons, we can place a 3σ upper limit of $\sim 0.38 \times 10^{-3}$ cts s^{-1} to the count rate at which the source would be statistically significant above the background. For the same spectral parameters as above, this translates into a (0.1–10) keV luminosity $\simeq 2 \times 10^{38}$ erg s^{-1} as a 3σ upper limit during Obs. 1 (ranging from 1.5 to 2.4 $\times 10^{38}$ erg s^{-1} for $\Gamma = 1$–2).

For the detection in Obs. 2 we proceeded as follows: if r_1 does indeed correspond to diffuse emission from the core of the galaxy, then the source contribution to r_2 will be $r_{\rm src} = (0.63 \pm 0.2)$ cts s^{-1}. Again, adopting the same spectral parameters as above, $r_{\rm src}$ translates into a (0.1–10) keV luminosity of $\sim 2.7 \times 10^{38}$ erg s^{-1} in Obs. 2, consistent with the low-luminosity detections reported by Brightman et al. (2016). Indeed, when combined with those observations, our result strengthens the case for the lower (least conservative) upper limit discussed above for Obs. 1.

Two main conclusions can be drawn from our analysis of these additional *Chandra* observations, in combination with those reported by Brightman et al. (2016). The first is that the source is highly variable, ranging from a maximum luminosity $L_{\rm peak} \gtrsim 10^{40}$ erg s^{-1} down to a minimum of $L_{\rm min} \sim (2$–$3) \times 10^{38}$ erg s^{-1} (for a distance of 3.3 Mpc) where it can still be detected. Below the latter value, the background emission from the host galaxy becomes dominant and it is extremely hard to separate it from the emission of M82-X2. The second conclusion is that the source remained *undetected* in the first observation made with the HRC: we placed a very conservative upper limit of 4.4×10^{38} erg s^{-1} to the source luminosity during Obs. 1 – assuming that the entire count rate is due to the source – and a more stringent upper limit – based on a plausible assumption for the background – of $\sim 2 \times 10^{38}$ erg s^{-1}.

Whether this observed luminosity transition between Obs. 1 and 2 occurred in a continuous fashion or in a sharp step remains to be determined in the future, through deeper and less sparse observations of the source.

3 BASIC PROPERTIES OF MAGNETICALLY THREADED DISCS

When accretion occurs on to a magnetic NS, the interaction between the accreting material and the NS magnetosphere affects the system dynamics in several ways. For disc accretion, in particular, the main elements can be briefly summarized as follows.

(i) The accreting plasma is threaded – at least partially – by the stellar magnetic field. The inner disc is truncated by the resulting magnetic stresses at a distance r_m from the NS. It is customary to write this truncation radius in terms of the classical Alfvén radius for spherical accretion, $r_{\rm A}$, with the simple expression $r_m \simeq \xi r_{\rm A}$, where $\xi < 1$. The Alfvén radius is where the magnetic pressure equals the ram pressure of the infalling material. It depends on the mass accretion rate, $\dot{M}$, and on the NS mass, radius, and magnetic moment.[2] For disc accretion, on the other hand, angular momentum balance is the most relevant constraint (see e.g. Ghosh & Lamb 1979b; Wang 1996). At decreasing radii, the magnetic stress grows faster than the viscous/material one: once it becomes dominant, it disrupts the disc forcing matter to fall along magnetic field lines. This difference is simply encoded in the parameter ξ, the value of which is only weakly constrained: on observational grounds, a number of studies have indicated $\xi \sim (0.3$–$1)$ as a conservative estimate of the range of variation (Psaltis & Chakrabarty 1999). Theoretically, the semi-analytic model by Ghosh & Lamb (1979a, hereafter GL79), and recent numerical simulations (Romanova et al. 2002, 2003, 2004) indicate a value $\xi \approx 0.5$, with only a very weak dependence on $\dot{M}$, if any. In an alternative semi-analytic model, Erkut & Alpar (2004) estimate values of $\xi \sim 0.35$–1.2 in different sources, or even in the same source at different accretion stages. In an independent approach to the problem, Wang (1987, 1996) argued for a value of $\xi \gtrsim 1$; Bozzo et al. (2009) extended Wang's approach and showed that, in this model, r_m is almost independent of the mass accretion rate, over a wide range of values of $\dot{M}$. The relation

[2] In more detailed calculations (e.g. Ghosh 1996, 2007) small corrections to this simple functional form were derived. These have only a minor effect on our estimates and, for the sake of simplicity, will be neglected in the following.

Downloaded from https://academic.oup.com/mnras/article-abstract/457/3/3076/2588907 by guest on 29 April 2020

with r_A in this case is more complex, involving an $\dot{M}$-dependent ξ (Section 4.3).

(ii) The inner edge of the disc, r_m, depends on the total pressure inside the disc, which has a contribution from both gas and radiation. The relative importance of the latter grows at smaller radii, at a fixed mass accretion rate, as more energy is locally released inside the disc. In particular, for a given $\dot{M}$, one can define a transition radius, r_{tr}, inside which radiation pressure dominates over gas pressure (e.g. Frank, King & Raine 2002):

$$r_{tr} \approx 7.5 \times 10^7 \mathrm{cm} \left(\frac{\alpha}{0.1}\right)^{2/21} \left(\frac{\dot{M}}{\dot{M}_E}\right)^{16/21} \left(\frac{M}{1.4\,\mathrm{M}_\odot}\right)^{1/3}, \quad (1)$$

where α is the usual viscosity parameter and the Eddington mass accretion rate is $\dot{M}_E = 4\pi\sigma_T m_p R/c \approx 1.75 \times 10^{-8}\,\mathrm{M}_\odot\ \mathrm{yr}^{-1}$, with the corresponding Eddington luminosity $L_E = GM\dot{M}_E/R \simeq 1.75 \times 10^{38}$ erg s^{-1}, for a 1.4 $\mathrm{M}_\odot$ NS with a radius $R = 10$ km. As long as $r_{tr} < r_m$, only gas pressure is important in the disc. When $r_{tr} > r_m$, on the other hand, radiation pressure dominates the inner disc, where more energy is released and most of the disc–magnetosphere interaction occurs. Following this transition, a change in the functional form of r_m occurs and, in particular, a different dependence on $\dot{M}$ will ensue[3] (Ghosh 1996):

$$r_m^{(g)} = \xi \left(\frac{\mu^4}{2GM\dot{M}^2}\right)^{1/7} \quad \text{gas-pressure regime}$$
$$r_m^{(r)} = A \left(\frac{\mu^4}{M\dot{M}}\right)^{1/7} \quad \text{radiation-pressure regime}, \quad (2)$$

where the magnetic dipole moment $\mu = B_p R^3/2$ and B_p is the field strength at the magnetic pole.[4] For consistency, the normalization, A, in $r_m^{(r)}$ is set so that the two expressions are equal at the transition radius, r_{tr}. As we will show in the next section, the weaker $\dot{M}$-dependence in radiation-pressure-dominated regions play an important role in NuSTAR J095551+6940.8.

(iii) The threading magnetic field regulates the exchange of angular momentum between the NS and the disc. This exchange is characterized by two regions separated at the corotation radius, $r_{co} = (GM/\Omega_s^2)^{1/3}$, where the Keplerian frequency equals the NS spin frequency, Ω_s. In the *inner region* matter rotates faster than the NS, thus exerting a spin-up torque as it gives up angular momentum to the NS magnetosphere. In the *outer region* matter rotates slower than the NS, thus causing spin-down as it gains angular momentum from the faster rotating magnetosphere. Depending on the strength of these two terms, the NS can either spin-up or down while accreting; in either case, the system naturally evolves towards *spin equilibrium*, in which the magnetic and material torques are at equilibrium and the NS accretes at constant period. This occurs when $r_m^{(eq)} \approx (0.5\text{–}0.9) r_{co}$, depending on poorly known microphysical details of the disc–magnetosphere interaction (GL79, Wang 1987, 1996; Yi, Wheeler & Vishniac 1997; Erkut & Alpar 2004; Parfrey, Spitkovsky & Beloborodov 2015). Spin equilibrium can be used to set a constraint on B_p, if a transition between spin-up and spin-down is observed: the luminosity at the transition yields the mass accretion rate at equilibrium, $\dot{M}_{eq}$, leaving only μ and ξ as unknowns in equation (2).

[3] The scaling with other physics parameters is mostly unaffected.

[4] Note that the above scalings cannot be used in the Wang model: we will show in Section 4.3, that this model can be described via a modified version of equation (2), with a specific $\dot{M}$-dependence of ξ that cancels out the one in the denominator.

(iv) The NS will be an *accretor* only if the disc extends inside the corotation radius, such that $r_m < r_{co}$. The accretion luminosity in this case is $L_{acc} \sim GM\dot{M}/R$. If, on the other hand, $r_m > r_{co}$, then matter cannot reach smaller radii than r_m: in approaching the faster rotating magnetosphere it acquires angular momentum and is thus forced outwards. This is the so-called *propeller regime*, in which accretion on to the NS is inhibited and a strong spin-down is expected. Since matters does not flow inside r_m, only half of its potential energy at $r_m (\geq r_{co})$ is released, the other half remaining as kinetic energy of the orbital motion. The propeller luminosity is therefore $L_{prop} \leq GM\dot{M}/(2r_{co})$.

4 LUMINOSITY VARIATIONS IN NUSTAR J095551+6940.8: MODEL CONSTRAINTS

In the following, we will use the observed luminosities of NuSTAR J095551+6940.8 to set constraints on the strength of the NS magnetic field and on the physical regime in the accretion disc.

The luminosity range over which the source is observed, from $L_{min}^{(ob)}$ to $L_{peak}^{(ob)}$, should correspond to the *accretor* phase, in which $r_m \lesssim r_{co}$ and the mass inflow proceeds all the way to the NS surface. Given the spin period and the magnetic dipole moment of the NS, this implies the existence of a minimum mass accretion rate, $\dot{M}_{min}$, below which r_m is larger than r_{co} and the NS enters the *propeller* regime.

The value of $\dot{M}_{min}$ and the associated luminosity, $L_{min}^{(th)}$, are determined by the condition $r_m \equiv r_{co}$. This requires that we first set the value of the coefficient ξ in equation (2), and then determine the pressure regime in the inner parts of the disc, which will select the appropriate expression for r_m. Given the uncertainties on ξ discussed in Section 3, we define here our 'reference' model as the one with $\xi = 0.5$, close to the results of recent numerical simulations. This will be used for the core of our argument (Section 4.1), but then we will discuss how our conclusions change if we let ξ vary within a wider range, from $\lesssim$0.3 to 1 (Section 4.2). We will also consider a specific model in which ξ depends explicitly on $\dot{M}$ (Section 4.3). At the end of Section 4 we will summarize our main conclusions, showing that they remain robust even using widely different models for the disc–magnetosphere coupling.

4.1 The 'reference model': $\xi = 0.5$

Using $\xi = 0.5$ in equation (2), we plotted in the two panels of Fig. 2 the ratio r_m/r_{co} as a function of the mass accretion rate, $\dot{M}/\dot{M}_E$, and the corresponding luminosity as a function of r_m/r_{co}, for four representative values of the dipole magnetic field. The upper and lower values allow a direct comparison of our conclusions with those of recent studies (Tsygankov et al. 2016; Brightman et al. 2016), as explained below. Note that L/L_E in the right-hand panel of Fig. 2 represents the luminosity $L_{acc} = GM\dot{M}/R$, in the accretor regime, and the luminosity $L_{prop} = GM\dot{M}/(2r_m)$ in the propeller regime (blue shaded area). Finally note that, at the accretor–propeller boundary, not only a jump in luminosity occurs (by a factor $R/2r_{co}$ in the ideal case) but all curves change their slope. This change is due to the fact that, while during accretion the luminosity depends linearly on $\dot{M}$, in the propeller regime the luminosity depends on the ratio $\dot{M}/r_m$, where $\dot{M}$ and r_m are related via equation (2). As a consequence, in propeller the power-law scaling of L with r_m decreases by one.

In the same figure we also show the transition radius, r_{tr}, as a grey dashed diagonal line: gas pressure dominates above that line, radiation pressure below it. Note that r_{tr}, hence the position of the grey dashed line, does not depend on the value of ξ. However, the

Downloaded from https://academic.oup.com/mnras/article-abstract/457/3/3076/2588907 by guest on 29 April 2020

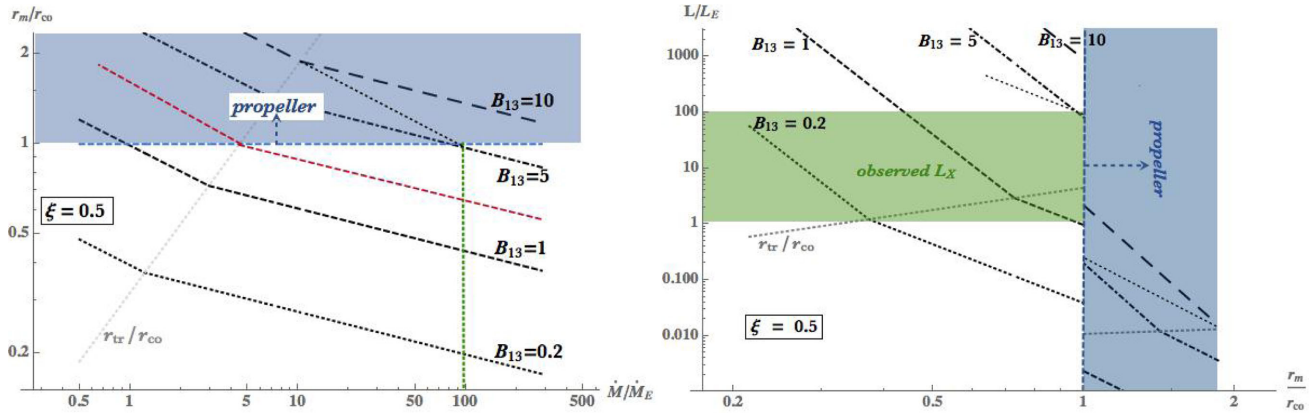

Figure 2. Left-hand panel: the ratio r_m/r_{co} as a function of the mass accretion rate (in Eddington units) for four values of the magnetic field strength. The region to the left of the grey dotted line is gas-pressure dominated, while the region to the right is radiation-pressure dominated. The green dashed vertical line indicates the mass accretion rate at the source peak luminosity (for isotropic emission). The red dotted curve highlights the 'special' case $B_{p,13} = 2$ (cf. Section 4.1). For illustration, the thin black dotted line shows the extrapolation of the gas-pressure-dominated curve in the case $B_{13} = 10$: this line reaches the boundary of the shaded blue area (propeller regime) at a significantly lower $\dot{M}$ than the solution which properly accounts for radiation-pressure effects. Right-hand panel: the source luminosity, in Eddington units, versus the ratio r_m/r_{co}, for the same four magnetic dipole fields. The thin dotted black line illustrates again the case $B_{13} = 10$ if radiation-pressure effects are neglected: only under this approximation the accretor regime can be reached at a sufficiently low luminosity to match the peak luminosity of NuSTAR J095551+6940.8.

value of the accretion rate at this transition, $\dot{M}_{tr}$, and of the associated luminosity, L_{tr}, are obtained from the equality $r_m^{(g)} = r_{tr}$, and thus depend (almost linearly) on ξ. In Eddington units we obtain

$$\frac{\dot{M}_{tr}}{\dot{M}_E} = \frac{L_{tr}}{L_E} \approx 3 B_{p,13}^{6/11} (\xi/0.5)^{21/22} \frac{R_6^{18/11}}{M_{1.4}^{3/22}}, \quad (3)$$

where $Q_x = Q/10^x$ and $M_{1.4} \equiv M/(1.4\,M_\odot)$. By substituting $\dot{M}_{tr}$ in the condition $r_m^{(r)} = r_m^{(g)}$ one can fix the factor A in equation (2), obtaining $r_m^{(r)} = r_m^{(g)} (\dot{M}/\dot{M}_{tr})^{1/7}$.

Note that even the line showing r_{tr}/r_{co} has a jump, and a marked change in slope, at the accretor–propeller boundary, since $\dot{M}(L)$ is discontinuous there as discussed above. This line flattens in propeller because in accretion it has a positive index larger than 1, contrary to all other curves that become steeper, since their index was already negative in accretion.

Before describing in detail our results, three general conclusions can be drawn from the previous analysis:

(1) If $B_{p,13} \lesssim 2$, the condition $r_m = r_{co}$ is reached in the gas-pressure-dominated regime. This results from $L_{min}^{(g)} < L_{tr}$, which readily yields $B_{p,13} < 2(\xi/0.5)^{-7/4} M_{1.4}^{35/96} R_6^{-37/16} (P_s/1.37)^{77/48}$. In this regime, the minimum accretion luminosity is

$$\frac{L_{min}^{(g)}}{L_E} \approx 0.96 B_{p,13}^2 \left(\frac{\xi}{0.5}\right)^{7/2} \left(\frac{P_s}{1.37}\right)^{-7/3} \frac{R_6^5}{M_{1.4}^{2/3}}. \quad (4)$$

(2) If $B_{p,13} > 2$, on the other hand, the disc is already radiation-pressure dominated at the propeller–accretor transition. In this case, the minimum luminosity has an even stronger dependence on the magnetic field, scaling like B_p^4, and is shifted towards larger values compared to the extrapolation of the gas-pressure-dominated case.

(3) If $B_{p,13} < 2$, the flattening of the $\dot{M}$-dependence of r_m beyond $\dot{M}_{tr}$ favours a much wider range of accretion luminosities than the standard $r_m \propto \dot{M}^{-2/7}$ scaling. On the contrary, the same flattening of the $\dot{M}$-dependence shrinks the range of accretion luminosities for NS with $B_{p,13} > 2$, because its effect is shifting the minimum upwards.

We can now look more closely at the behaviour of the solutions for three representative values of the magnetic field:

(i) For $B_{p,13} = 0.2$ the disc is radiation-pressure dominated at all accretion rates $\geq 1.1\dot{M}_E$, with the inner disc extending well inside the corotation radius. The observed luminosity range, ∼(1–100) L_E, corresponds to r_m varying between $\approx 0.2 r_{co}$ and $\approx 0.4 r_{co}$, always in the radiation-pressure-dominated regime. Very close to the observed minimum, $L_{min}^{(ob)} \simeq 1.1 L_E \approx 2 \times 10^{38}$ erg s^{-1}, gas pressure takes over while the NS remains an accretor for further decreasing values of $\dot{M}$, until the transition to propeller occurs at $L_{min}^{(th)} \approx 0.044 L_E (B_{p,12}/2)^2 (\xi/0.5)^{7/2} (P_s/1.37s)^{-7/3}$. Due to the background emission from the host galaxy and the neighbouring sources, it will be observationally very challenging to track the source at these low luminosities; however, no sharp transition below the currently observed minimum is expected in this case.

At the same time, the high peak luminosity of the source would require a significant beaming if $B \sim 10^{12}$ G, since in this case there is no obvious way to exceed the Eddington limit by a large factor. In fact, a beaming ∼0.2 would also reconcile the measured $\dot{P} \simeq 2 \times 10^{-10}$ with the (beaming-corrected) luminosity. Explaining such a beaming *of the pulsed emission* represents a problem on its own (see discussion in paper I). In addition, this scenario encounters an even greater difficulty in the large $\dot{P}$-fluctuations measured while the source was near its peak emission (Bachetti et al. 2014). This strongly suggest that the NS was close to spin equilibrium at that epoch (paper I), while the result $r_m \simeq 0.2 r_{co}$ at the peak is hardly consistent with spin equilibrium, being largely below the range $r^{(eq)} \approx (0.5–0.95) r_{co}$ provided by all existing theoretical estimates. Therefore, a new explanation would also be required for the large $\dot{P}$ fluctuations.

(ii) For $B_{p,13} = 1$, radiation pressure dominates the inner disc at $L_X \geq 3 L_E$, which corresponds to $r_m \leq 0.8 r_{co}$; as expected, the disc is gas-pressure dominated at the minimum luminosity, $L_{min}^{(g)} \approx 1.7 \times 10^{38}$ erg s^{-1} (cf. equation 4), similar to the upper limit determined in Section 2.

Downloaded from https://academic.oup.com/mnras/article-abstract/457/3/3076/2588907 by guest on 29 April 2020

It is therefore a natural prediction that a NS with $P_s = 1.37$ s would be detectable as an accreting source down to $\sim 2 \times 10^{38}$ erg s^{-1} *if it had a magnetic dipole*[5] $B \sim 10^{13}$ G.

Once in propeller, the luminosity will be much lower since now the accretion radius will be r_{co} instead of R (e.g. Corbet 1996). In the case of an 'ideal' (i.e. sharp) transition, the source luminosity should drop suddenly by a factor $R/2r_{co} \sim 1/400$, which is determined almost entirely by the spin period (see the right-hand panel of Fig. 2): even in a more realistic and smoother transition, a significant drop in luminosity must be expected just below the currently observed minimum (e.g. Romanova et al. 2003). More generally, an observational determination of L_{min} would allow a robust estimate of the magnetic field strength. In the observations discussed in Section 2 the source was undetected, with a 3σ upper limit on its luminosity of $\approx 10^{38}$ erg s^{-1}, consistent with $L^{(g)}_{min}$ derived above: this limit can only be improved with future X-ray detectors having at least the same angular resolution of *Chandra* and a much larger collecting area (to achieve the required limit within reasonable exposure times), given the high and highly patchy background in the source region.

In addition, when $B \sim 10^{13}$ G the Eddington limit is significantly modified by the magnetically reduced electron scattering cross-section, which gives a maximum luminosity $L^{(th)}_{peak} \sim 10^{40} B_{13}^{4/3}$ erg s^{-1} (Paczynski 1992). This value matches well the observed peak luminosity of NuSTAR J095551+6940.8 (cf. paper I) that, as shown in Fig. 2, is naturally reached when $r_m \gtrsim 0.45 r_{co}$, a condition that is well consistent with spin equilibrium.

(iii) For $B_p > 5 \times 10^{13}$ G, the equality $r_m^{(r)} = r_{co}$ implies that the system is in the propeller regime at all accretion rates lower than $\sim 85 \dot{M}_E (B_{p,13}/5)^4$. This limit is $\gtrsim 3$ times higher than what would have been obtained using $r_m^{(g)}$, and is a direct consequence of the transition to radiation-pressure dominance which occurs above $\dot{M} \sim 7.5 \dot{M}_E$. This is illustrated in both panels of Fig. 2 by the black thin dotted line, which represents the extrapolation of $r_m^{(g)}$ beyond its limit of validity for the case $B_p = 10^{14}$ G.

This 'high-field case' is the most problematic in light of current observations. The NS can only enter the accretor regime at a minimum luminosity $L^{(th)}_{min} \approx 1.7 \times 10^{40}$ erg s^{-1} or higher, as a consequence of radiation pressure dominating the inner disc, thus violating two constraints at a time: on the one hand, $L^{(th)}_{min}$ would exceed the observed peak luminosity of the source if $B_p > 5 \times 10^{13}$ G and, on the other hand, all intermediate states in which the source has a luminosity $\sim$a few $\times 10^{39}$ erg s^{-1} would be impossible to account for, since in propeller the source would have a luminosity $L_{prop} \sim 6 \times 10^{37}$ erg s^{-1}. A stronger field would only exacerbate this problem, given that $L^{(th)}_{min}$ scales with B_p^4 in the radiation-pressure-dominated regime.

We stress again the crucial role of radiation-pressure effects for our conclusions. If $B_p \gtrsim 2 \times 10^{13}$ G (i.e. above the red dashed line in Fig. 2), not accounting for such effects would allow the NS to enter the accretor regime at a significantly lower luminosity, leading to the apparent conclusion that a field $\gtrsim 10^{14}$ G can be consistent with the peak luminosity of NuSTAR J095551+6940.8 (Tsygankov et al. 2016).

[5] Recently Brightman et al. (2015) have concluded that B larger than $\sim 10^{12}$ G would be inconsistent with the lower luminosity states at which M82-X2 is detected. However, this result stems from the assumption of spherical accretion (Stella et al. 1986) and neglecting radiation pressure effects (in our notation, this corresponds to the extreme value $\xi = 1$).

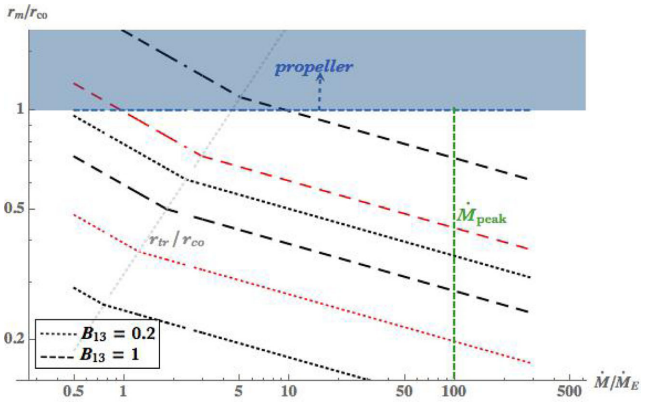

Figure 3. Same as in the left-hand panel of Fig. 2, but for different values of the parameter ξ. For each value of the magnetic field, i.e. dashing style, the lower black curve is obtained for $\xi = 0.3$ and the upper one for $\xi = 1$. The red curves show instead the results of Fig. 2, obtained with the reference value $\xi = 0.5$.

To summarize, we have shown that a NS with $B \sim 10^{13}$ G is sufficient to interpret the observational properties of NuSTAR J095551+6940.8 in a straightforward fashion: its peak luminosity, the minimum luminosity at which it is observed and the non-detections below that value. In addition, it was already shown that this case can also explain the measured value of $\dot{P}$ and its fluctuations around the peak luminosity (see paper I).

A lower field strength might not be excluded – although significantly lower B-fields require a high degree of fine-tuning (see paper I). A B-field significantly larger than 10^{13} G would not match the luminosity range over which the source is observed and can be ruled out.

4.2 Constant ξ models: dependence on ξ-values

We next explore the dependence of our results on the parameter ξ. Given the linear dependence of r_m on ξ, for the same magnetic field strength, a larger ξ will push the system in the propeller phase at larger values of $\dot{M}$. Correspondingly, the minimum luminosity at which the system can be in the accretion phase will be larger for larger ξ, given a fixed B-field strength. This is clear from the dependence of $L^{(th)}_{min}$ on ξ in equation (4), and is shown in Fig. 3 for the two limiting cases $\xi = 0.3$ and $\xi = 1$. The dependence of $\dot{M}_{tr}$ on ξ (equation 3) is due to the shifting position of the r_m curves.

Conversely, we can rewrite equation (4) as a relation between the magnetic dipole of the source and the value of ξ, if we know the minimum luminosity at which the NS can accrete. Recalling that equation (4) holds for $B_{p,13} \lesssim 2$, we obtain

$$B_{p,13} \simeq \left[\frac{L^{(g)}_{min}}{L_E}\right]^{1/2} \left(\frac{\xi}{0.5}\right)^{-7/4} \left(\frac{P_s}{1.37s}\right)^{7/6} \frac{M_{1.4}^{1/3}}{R_6^{5/2}}. \quad (5)$$

If we now assume for $L^{(g)}_{min}$ the minimum luminosity $L^{(ob)}_{min} \approx 10^{38}$erg s^{-1} determined with current observations (Section 2), then from equation (5) we obtain $B_{13} \sim$ (0.4–3) for ξ in the (1–0.3) range, very similar to the 'high-B case' discussed in paper I. These numbers can be easily adjusted if future observations will be able to determine the minimum luminosity with better accuracy: note, however, that the estimated magnetic field strength scales only with the square root of the minimum accretion luminosity.

Downloaded from https://academic.oup.com/mnras/article-abstract/457/3/3076/2588907 by guest on 29 April 2020

4.3 Wang model: a specific prescription for $\xi(\dot{M})$

Wang (1987, 1995, 1996) derived the inner disc radius from the condition $r_m^2 B_z(r_m) B_\phi(r_m) = \dot{M}\left[d/dr\left(r^2\Omega_K\right)\right]_{r_m}$, i.e. that the magnetic stress is equal to the material stress in the disc.[6] Adopting different phenomenological prescriptions for the growth and dissipation of the toroidal field in the disc, the radial profile of $B_\phi(r)$ can be calculated and, hence, the value of r_m as a function of the NS magnetic field, the mass accretion rate and several microphysics parameters that are poorly constrained from both theory and observations.

This model predicts that, at spin equilibrium, the inner disc radius is close to the corotation radius ($r_m^{(\rm eq)} \gtrsim 0.9 r_{\rm co}$), nearly independent of the phenomenological prescriptions adopted for the toroidal field in the disc (Wang 1995). Bozzo et al. (2009) generalized this approach, deriving expressions for $x = r_m/r_{\rm co}$ in Wang-type models with various prescriptions for the mechanisms by which the toroidal field is damped. Here we consider two cases, which bracket the (small) range of possible variations: (*a*) the winding of the field lines threading the disc is limited by magnetic reconnection taking place in the magnetosphere; (*b*) the amplification of the toroidal field is damped by diffusive decay due to turbulent mixing within the disc.

$$x^{-7/2} - x^{-2} = 4.17\times10^{-3}\frac{M_{1.4}^{5/3}P^{7/3}\dot{M}_{16}}{\gamma_{\rm max}\eta^2\mu_{30}^2} \qquad (a)$$

$$x^{-7/2} - x^{-2} = 4.17\times10^{-3}\frac{\alpha}{\gamma}\frac{M_{1.4}^{5/3}P^{7/3}\dot{M}_{16}}{\eta^2\mu_{30}^2} \qquad (b)\,. \qquad (6)$$

In the above, α is the usual viscosity coefficient, $\gamma = B_\phi/B_z$ is the magnetic pitch angle in the disc and $\gamma_{\rm max}$ its maximum value compatible with magnetic reconnection out of the disc plane, and η the factor by which the NS magnetic field is screened by electric currents flowing in the disc. These parameters are subject to significant uncertainties, that make it difficult to draw quantitative conclusions. However, such uncertainties can be bypassed if a transition between spin-up and spin-down is observed (Bozzo et al. 2009), since the transition signals the point of spin equilibrium. When expressed in terms of the equilibrium quantities, $\dot{M}_{\rm eq}$ (observed) and $x^{(\rm eq)}$ (fixed by the model), equation (6) give x as a function of $\dot{M}$ and show that r_m remains $\lesssim r_{\rm co}$, nearly constant for $\dot{M} < \dot{M}_{\rm eq}$. In particular, accretion on to the NS continues even at the smallest values of $\dot{M}$, and is never quenched by the propeller. This apparently unphysical behaviour makes it impossible, within the framework of Wang-type models, to constrain the NS properties from luminosity variations. However, we can use equation (6) to estimate the NS magnetic field based on the assumption that a spin-up–spin-down transition, or a very close approach to spin equilibrium, was observed in NuSTAR J095551+6940.8. This assumption is motivated by the large torque fluctuations measured by Bachetti et al. (2014), when the source was close to its peak luminosity (cf. paper I). We thus set[7] $\dot{M}_{\rm eq} \approx 50\dot{M}_E$, and use the value $x^{(\rm eq)} \simeq 0.967(0.915)$ for case $a(b)$ in equation (6) to obtain

$$B_{p,13} \approx \frac{5.4}{\eta\gamma_{\rm max}^{1/2}}\left(\frac{\dot{M}_{\rm eq}}{50\dot{M}_E}\right)^{1/2} P_{1.37}^{7/6}\frac{M_{1.4}^{5/6}}{R_6^3} \qquad (a)$$

$$B_{p,13} \approx \frac{1.2\alpha_{0.1}^{1/2}}{\eta\gamma^{1/2}}\left(\frac{\dot{M}_{\rm eq}}{50\dot{M}_E}\right)^{1/2} P_{1.37}^{7/6}\frac{M_{1.4}^{5/6}}{R_6^3} \qquad (b)\,. \qquad (7)$$

These results are again in overall agreement with those of the previous sections and of paper I: as a general conclusion, the estimated $\sim10^{13}$ G B-field appears robust against a variety of independent arguments and adopted models. Note that, since $\eta < 1$ and $\gamma \gtrsim 1$, slightly larger values of the magnetic field may possibly be favoured by Wang-type models.

Using the magnetic fields of equation (7) we can calculate $r_{\rm A}$ and, since $r_m \lesssim r_{\rm co}$ when $\dot{M} \lesssim \dot{M}_{\rm eq}$, we obtain $r_m/r_{\rm A} \sim (0.25\text{–}0.55)$ in NuSTAR J095551+6940.8, for $\dot{M} = (\dot{M}_E - \dot{M}_{\rm eq})$. Equation (6) also imply that r_m starts decreasing approximately like $r_{\rm A}$ if $\dot{M} > \dot{M}_{\rm eq}$ (Bozzo et al. 2009): therefore, ξ remains $\gtrsim$0.55 when $\dot{M}$ is above the equilibrium value. As a conclusion, Wang's model may be cast in the form $r_m = \xi(\dot{M})r_{\rm A}$, where the numerical value of the function $\hat{\xi}(\dot{M})$ ranges in the lower half of the interval considered in the previous sections. This is consistent with our discussion of Section 4.2, that lower values of ξ tend to favour larger values of the NS magnetic field.

5 SUMMARY AND DISCUSSION

The wide spread of luminosities of NuSTAR J095551+6940.8 (M82-X2) , encompassing a range from highly super-Eddington, to $\sim$ Eddington to no detection, has allowed us to investigate various physically interesting accretion regimes for a magnetized NS.

Here, we have extended the analysis of archival *Chandra* data with the inclusion of two HRC observations. The source is detected in one of them, with an estimated luminosity $\sim2.6\times10^{38}$ erg s^{-1}. On the other hand, the source is *undetected* in the first HRC observation, during which it is indistinguishable from the diffuse emission of the host galaxy. This non-detection yields a conservative upper limit of $L_{u.l.}^{(a)} \gtrsim 4.4\times10^{38}$ erg s^{-1} to the source luminosity, assuming that the background contribution to the counts from the M82-X2 region is negligible. On the other hand, by assuming that those counts are mostly due to the background – as suggested by the count rate being the same as in nearby background regions – we placed a more stringent upper limit of $L_{u.l.}^{(b)} \simeq 2\times10^{38}$ erg s^{-1} to the source luminosity.

We performed an in-depth analysis of the large luminosity variations of NuSTAR J095551+6940.8 (M82-X2), within a magnetically threaded disc model, including the transition of the inner disc between gas-pressure and radiation-pressure dominance across the various accretion states. We explored a range of models characterized by different prescriptions for the location of the disc truncation radius, and found that the NS magnetic field should be in the (0.4–3) $\times10^{13}$ G range, with a favoured value of $\sim10^{13}$ G, if accretion on to the NS becomes inhibited below a luminosity $\simeq L_E$. The latter value is fully compatible with the currently determined minimum luminosity of the source, and with the upper limit $L_{u.l.}^{(b)}$ discussed above. The estimated B-field is consistent with the conclusions of paper I, which were based on independent arguments.

[6] The same condition is also considered in the GL model. However, in this model the radial rotation profile $\Omega(r)$ is allowed to deviate from Keplerian in a narrow boundary layer, before reaching the inner disc edge in corotation with the magnetosphere. This different treatment results in a different location of the inner disc edge in the GL model and a more pronounced dependence of r_m on the mass accretion rate.

[7] In paper I it was shown that the spin-up–spin-down transition is likely to occur at luminosities somewhat smaller than the peak. Hence, we set for reference this transition at half the peak, i.e. at 50 $\dot{M}_E$. Note the weak dependence of the estimates in equation (7) on the exact value of this parameter.

Downloaded from https://academic.oup.com/mnras/article-abstract/457/3/3076/2588907 by guest on 29 April 2020

In our analysis, the estimated magnetic field has a degeneracy with the poorly constrained value of ξ, the ratio between the disc truncation radius and the Alfvén radius. An independent determination of the NS B-field might in principle break this degeneracy, allowing to place interesting constraints on ξ, hence on the viability of different models for the disc–magnetosphere coupling. In accreting X-ray pulsars, one possible way to estimate the NS magnetic field is via a high-energy break in the emission spectrum, which is known to correlate with the cyclotron energy. However, the cyclotron resonance shifts to progressively lower energies in several bright X-ray pulsars, as the accretion luminosity grows and approaches the Eddington limit. This shift is attributed to the increasing height of the accretion column above the NS surface, which therefore samples regions of progressively decreasing B-field strength (Becker et al. 2012, and references therein). In NuSTAR J095551+6940.8, a spectral break at ∼14 keV was detected when the source was close to its peak emission (Brightman et al. 2016): taken at face value, this is consistent with the break observed in several accreting NS with $B \sim 10^{12}$ G. However, we note that NuSTAR J095551+6940.8 is an extremely bright X-ray pulsar in an unprecedented accretion regime. If this trend, and the correlation between cyclotron energy and spectral break, were to continue into the super-Eddington regime, then $B_p \sim 10^{13}$ G may well be consistent with the finding of Brightman et al. (2016). In fact, revealing a shift in the spectral break energy of NuSTAR J095551+6940.8 when the source is at different luminosities would provide significant support to this idea.

ACKNOWLEDGEMENTS

SD was partially supported by an SFB/Transregio 7, funded by the Deutsche Forschungsgemeinschaft (DFG). RP and SD acknowledge partial support by *Chandra* grant (awarded by SAO) ARS-16005X. AP acknowledges partial support from 'NewCompStar', COST Action MP1304.

REFERENCES

Bachetti M. et al., 2014, Nature, 514, 202
Becker P. A. et al., 2012, A&A, 544, A123
Bozzo E., Stella L., Vietri M., Ghosh P., 2009, A&A, 493, 809
Brightman M. et al., 2016, ApJ, 816, 60
Christodoulou D. M., Laycock S. G. T., Kazanas D., 2014, preprint (arXiv:1411.5434)
Chiang Y.-K., Kong A. K. H., 2011, MNRAS, 414, 1329
Corbet R. H. D., 1996, ApJ, 457, L31
Dall'Osso S., Perna R., Stella L., 2015, MNRAS, 449, 2144 (Paper I)
Eksi K. Y., Anda I. C., Cikintoglu S., Gencali A. A., Gungor C., Oztekin F., 2015, MNRAS, 448, L40
Erkut M. H., Alpar M. A., 2004, ApJ, 617, 461
Foley R. et al., 2014, MNRAS, 443, 2887
Frank J., King A., Raine D., 2002, Accretion Power in Astrophysics. Cambridge Univ. Press, Cambridge
Freeman P. E., Kashyap V., Rosner R., Lamb D. Q., 2002, ApJS, 138, 185
Ghosh P., 1996, ApJ, 459, 244
Ghosh P., 2007, Rotation and Accretion Powered Pulsars: World Scientific Series in Astronomy and Astrophysics. World Scientific Press, Singapore.
Ghosh P., Lamb F. K., 1979a, ApJ, 234, 296 (GL79)
Ghosh P., Lamb F. K., 1979b, ApJ, 232, 259
Kluzniak W., Lasota J.-P., 2015, MNRAS, 448, L43
Lyutikov M., 2014, preprint (arXiv:1410.8745)
Parfrey K., Spitkovsky A., Beloborodov A. M., 2015, preprint (arXiv:1507.08627)
Psaltis D., Chakrabarty D., 1999, ApJ, 521, 332
Paczynski B., 1992, Acta Astron., 42, 145
Romanova M. M., Ustyugova G. V., Koldoba A. V., Lovelace R. V. E., 2002, ApJ, 578, 420
Romanova M. M., Toropina O. D., Toropin Yu. M., Lovelace R. V. E., 2003, ApJ, 588, 400
Romanova M. M., Ustyugova G. V., Koldoba A. V., Lovelace R. V. E., 2004, ApJ, 616, L151
Tong H., 2015, Astron. Nachr., 336, 835
Tsygankov S. S., Mushtukov A. A., Suleimanov V. F., Poutanen J., 2016, MNRAS, 457, 1101
Wang Y.-M., 1987, A&A, 183, 257
Wang Y.-M., 1995, ApJ, 449, L153
Wang Y.-M., 1996, ApJ, 465, L111
Yi I., Wheeler J. C., Vishniac E. T., 1997, ApJ, 481, L51

This paper has been typeset from a TEX/LATEX file prepared by the author.

Downloaded from https://academic.oup.com/mnras/article-abstract/457/3/3076/2588907 by guest on 29 April 2020